THE UNIVERSITY of EDINBURGH

Edinburgh Research Explorer

Destruction of the cosmic -ray emitter 26Al in massive stars: Study of the key 26Al (n,) reaction

Citation for published version:
n_TOF Collaboration, Lederer-Woods, C, Woods, PJ, Davinson, T, Estrade, A, Kahl, D & Lonsdale, SJ 2021, 'Destruction of the cosmic -ray emitter 26Al in massive stars: Study of the key 26Al (n,) reaction', *Physical Review C*, vol. 104, no. 3, L032803, pp. 1-6. https://doi.org/10.1103/PhysRevC.104.L032803

Digital Object Identifier (DOI):
10.1103/PhysRevC.104.L032803

Link:
Link to publication record in Edinburgh Research Explorer

Document Version:
Peer reviewed version

Published In:
Physical Review C

General rights
Copyright for the publications made accessible via the Edinburgh Research Explorer is retained by the author(s) and / or other copyright owners and it is a condition of accessing these publications that users recognise and abide by the legal requirements associated with these rights.

Take down policy
The University of Edinburgh has made every reasonable effort to ensure that Edinburgh Research Explorer content complies with UK legislation. If you believe that the public display of this file breaches copyright please contact openaccess@ed.ac.uk providing details, and we will remove access to the work immediately and investigate your claim.

OPEN ACCESS

Download date: 22. Dec. 2021

Destruction of the cosmic γ-ray emitter ^{26}Al in massive stars: study of the key ^{26}Al(n,α) reaction

C. Lederer-Woods,[1,a] P. J. Woods,[1] T. Davinson,[1] A. Estrade,[1,b] J. Heyse,[2] D. Kahl,[1,c] S. J. Lonsdale,[1] C. Paradela,[2] P. Schillebeeckx,[2] O. Aberle,[3] S. Amaducci,[4,5] J. Andrzejewski,[6] L. Audouin,[7] M. Bacak,[8,3,9] J. Balibrea,[10] M. Barbagallo,[11] F. Bečvář,[12] E. Berthoumieux,[9] J. Billowes,[13] D. Bosnar,[14] A. Brown,[15] M. Caamaño,[16] F. Calviño,[17] M. Calviani,[3] D. Cano-Ott,[10] R. Cardella,[3] A. Casanovas,[17] F. Cerutti,[3] Y. H. Chen,[7] E. Chiaveri,[3,13,18] N. Colonna,[11] G. Cortés,[17] M. A. Cortés-Giraldo,[18] L. Cosentino,[19] S. Cristallo,[20,21] L. A. Damone,[11,22] M. Diakaki,[9] C. Domingo-Pardo,[23] R. Dressler,[24] E. Dupont,[9] I. Durán,[16] B. Fernández-Domínguez,[16] A. Ferrari,[3] P. Ferreira,[25] F.J. Ferrer,[26,27] P. Finocchiaro,[19] V. Furman,[28] K. Göbel,[29] A. R. García,[10] A. Gawlik,[6] S. Gilardoni,[3] T. Glodariu[†],[30] I. F. Gonçalves,[25] E. González-Romero,[10] E. Griesmayer,[8] C. Guerrero,[18] F. Gunsing,[9,3] H. Harada,[31] S. Heinitz,[24] D. G. Jenkins,[15] E. Jericha,[8] F. Käppeler,[32] Y. Kadi,[3] A. Kalamara,[33] P. Kavrigin,[8] A. Kimura,[31] N. Kivel,[24] M. Kokkoris,[33] M. Krtička,[12] D. Kurtulgil,[29] E. Leal-Cidoncha,[16] H. Leeb,[8] J. Lerendegui-Marco,[18] S. Lo Meo,[34,4] D. Macina,[3] A. Manna,[4,5] J. Marganiec,[6,35] T. Martínez,[10] A. Masi,[3] C. Massimi,[4,5] P. Mastinu,[36] M. Mastromarco,[11] E. A. Maugeri,[24] A. Mazzone,[11,37] E. Mendoza,[10] A. Mengoni,[34] P. M. Milazzo,[38] F. Mingrone,[3] A. Musumarra,[19,39] A. Negret,[30] R. Nolte,[35] A. Oprea,[30] N. Patronis,[40] A. Pavlik,[41] J. Perkowski,[6] I. Porras,[42] J. Praena,[42] J. M. Quesada,[18] D. Radeck,[35] T. Rauscher,[43,44] R. Reifarth,[29] C. Rubbia,[3] J. A. Ryan,[13] M. Sabaté-Gilarte,[3,18] A. Saxena,[45] D. Schumann,[24] P. Sedyshev,[28] A. G. Smith,[13] N. V. Sosnin,[13] A. Stamatopoulos,[33] G. Tagliente,[11] J. L. Tain,[23] A. Tarifeño-Saldivia,[17] L. Tassan-Got,[7] S. Valenta,[12] G. Vannini,[4,5] V. Variale,[11] P. Vaz,[25] A. Ventura,[4] V. Vlachoudis,[3] R. Vlastou,[33] A. Wallner,[46] S. Warren,[13] C. Weiss,[8] T. Wright,[13] and P. Žugec[14,3]

(The n_TOF Collaboration (www.cern.ch/ntof))

[1]*School of Physics and Astronomy, University of Edinburgh, Peter Guthrie Tait Road, EH9 3FD Edinburgh, UK.*
[2]*European Commission, Joint Research Centre, Geel, Retieseweg 111, B-2440 Geel, Belgium*
[3]*European Organization for Nuclear Research (CERN), Switzerland*
[4]*Istituto Nazionale di Fisica Nucleare, Sezione di Bologna, Italy*
[5]*Dipartimento di Fisica e Astronomia, Università di Bologna, Italy*
[6]*University of Lodz, Poland*
[7]*Institut de Physique Nucléaire, CNRS-IN2P3, Univ. Paris-Sud, Université Paris-Saclay, F-91406 Orsay Cedex, France*
[8]*Technische Universität Wien, Austria*
[9]*CEA Irfu, Université Paris-Saclay, F-91191 Gif-sur-Yvette, France*
[10]*Centro de Investigaciones Energéticas Medioambientales y Tecnológicas (CIEMAT), Spain*
[11]*Istituto Nazionale di Fisica Nucleare, Sezione di Bari, Italy*
[12]*Charles University, Prague, Czech Republic*
[13]*University of Manchester, United Kingdom*
[14]*Department of Physics, Faculty of Science, University of Zagreb, Zagreb, Croatia*
[15]*University of York, United Kingdom*
[16]*University of Santiago de Compostela, Spain*
[17]*Universitat Politècnica de Catalunya, Spain*
[18]*Universidad de Sevilla, Spain*
[19]*INFN Laboratori Nazionali del Sud, Catania, Italy*
[20]*Istituto nazionale di Astrofisica - Osservatorio Astronomico d'Abruzzo, Italy*
[21]*Istituto Nazionale di Fisica Nucleare, Sezione di Perugia, Italy*
[22]*Dipartimento di Fisica, Università degli Studi di Bari, Italy*
[23]*Instituto de Física Corpuscular, CSIC - Universidad de Valencia, Spain*
[24]*Paul Scherrer Institut (PSI), Villingen, Switzerland*
[25]*Instituto Superior Técnico, Lisbon, Portugal*
[26]*Centro Nacional de Aceleradores (U. Sevilla, J. Andaluca, CSIC), Avda Tomas A Edison, 7, 41092 Sevilla, Spain*
[27]*Departamento de FAMN, Univ. Sevilla. Aptdo 1065, 41012 Sevilla, Spain*
[28]*Joint Institute for Nuclear Research (JINR), Dubna, Russia*
[29]*Goethe University Frankfurt, Germany*
[30]*Horia Hulubei National Institute of Physics and Nuclear Engineering, Romania*
[31]*Japan Atomic Energy Agency (JAEA), Tokai-mura, Japan*
[32]*Karlsruhe Institute of Technology, Campus North, IKP, 76021 Karlsruhe, Germany*
[33]*National Technical University of Athens, Greece*
[34]*Agenzia nazionale per le nuove tecnologie (ENEA), Bologna, Italy*

[35]Physikalisch-Technische Bundesanstalt (PTB), Bundesallee 100, 38116 Braunschweig, Germany
[36]Istituto Nazionale di Fisica Nucleare, Sezione di Legnaro, Italy
[37]Consiglio Nazionale delle Ricerche, Bari, Italy
[38]Istituto Nazionale di Fisica Nucleare, Sezione di Trieste, Italy
[39]Dipartimento di Fisica e Astronomia, Università di Catania, Italy
[40]University of Ioannina, Greece
[41]University of Vienna, Faculty of Physics, Vienna, Austria
[42]University of Granada, Spain
[43]Department of Physics, University of Basel, Switzerland
[44]Centre for Astrophysics Research, University of Hertfordshire, United Kingdom
[45]Bhabha Atomic Research Centre (BARC), India
[46]Australian National University, Canberra, Australia

(Dated: September 20, 2021)

Neutron destruction reactions of the cosmic γ-ray emitter ^{26}Al are of importance to determine the amount of ^{26}Al ejected into our galaxy by supernova explosions, and for ^{26}Al production in Asymptotic Giant Branch (AGB) stars. We performed a new measurement of the ^{26}Al(n,α) reaction up to 160 keV neutron energy at the neutron time-of-flight facilities n_TOF at CERN and GELINA at EC-JRC. We provide strengths for 10 resonances, 6 of them for the first time. We use our data to calculate astrophysical reactivities for stellar temperatures up to 0.7 GK. Our results resolve a discrepancy between the two previous direct measurements of this reaction, and indicate higher stellar destruction rates than the most recently recommended reactivity.

PACS numbers: 25.40.Lw, 29.30.Hs, 27.80.+w

Radioactive ^{26}Al ($T_{1/2} = 7 \times 10^5$ years) was the first cosmic γ-ray emitter observed in our galaxy. Understanding the origins of ^{26}Al gives crucial information on nucleosynthesis processes in stars, the chemical evolution of our galaxy as well as the birth of our solar system. Galactic ^{26}Al was observed for the first time by the HEAO-3 (High Energy Astronomy Observatory) satellite mission [1] by detecting the characteristic 1.8-MeV γ-decay radiation. Later, more detailed satellite observations by COMPTEL on board CGRO and SPI on board INTEGRAL indicated that ^{26}Al is mainly produced in massive stars [2, 3]. Stellar models suggest ^{26}Al is produced during three different phases of stellar evolution [4–6]: (i) H core burning in Wolf-Rayet stars ($M > 30M_\odot$) [7], where ^{26}Al gets ejected into the interstellar medium by stellar winds, (ii) convective carbon shell burning and (iii) explosive C/Ne burning in massive stars, ejecting ^{26}Al during the subsequent core collapse supernova explosion. Final ^{26}Al yields sensitively depend on nuclear reaction rates producing and destroying ^{26}Al. Iliadis et al. [5] studied the effect of varying nuclear reaction rates on the final abundances of the ^{26}Al produced in the different stellar environments. Stellar ^{26}Al(n,α) and ^{26}Al(n,p) reaction rates between 1.1 and 2.3 GK (1 GK=10^9 K) were identified among the most important uncertainties impacting on ^{26}Al abundances in in hydrostatic and explosive carbon burning of massive stars.

^{26}Al may also be produced in Asymptotic Giant Branch stars, which are candidates for polluting the early solar system with it [8]. Hence, accurate data on ^{26}Al(n,α) and ^{26}Al(n,p) reaction rates around 0.3 GK are required to estimate their contribution to ^{26}Al abundances in the early solar system.
Our collaboration recently reported a new measurement of the ^{26}Al(n,p) reaction cross section [9]. There is only limited experimental data available for the ^{26}Al(n,α) reaction and that data is in disagreement. A new measurement is therefore required. We measured the ^{26}Al(n,α) reaction at two neutron time-of-flight facilities, the n_TOF facility at CERN, and the Geel Linear Accelerator GELINA situated at the European Commission Joint Research Center (EC-JRC) in Geel, Belgium.

The ^{26}Al(n,α) reaction induced by low energy neutrons produces ^{23}Na either in its ground state, here denoted as ^{26}Al(n,α_0), or in its first excited state at 0.44 MeV, here denoted as ^{26}Al(n,α_1). The first direct measurement of the ^{26}Al$(n,\alpha_0)^{23}$Na reaction was conducted by Koehler et al. [10] at the Los Alamos Neutron Science Center (LANSCE), covering neutron energies from thermal (0.0253 eV) to 10 keV. Koehler et al. detected α events using a set of silicon surface barrier detectors, and reported one large resonance in the cross section at 5.6 keV laboratory neutron energy. Later, the ^{26}Al(n,α_0) and ^{26}Al(n,α_1) reactions were studied by De Smet et al. [11] with an ionization chamber at GELINA. In this work resonances of ^{26}Al+n were identified up to a neutron energy of 110 keV and resonance strengths were extracted up to 42 keV neutron energy. The lowest lying resonance reported at a neutron energy of 5.9 keV had a lower resonance strength than the value reported in Ref. [10] (see

[a]corresponding author: claudia.lederer-woods@ed.ac.uk
[b]Present address: Central Michigan University, USA
[c]Present address: Extreme Light Infrastructure – Nuclear Physics, Horia Hulubei National Institute for R&D in Physics and Nuclear Engineering (IFIN-HH), 077125 Bucharest-Măgurele, Romani

Table I). Accordingly, the astrophysical reaction rates using the De Smet data are a factor of ≈ 1.7 smaller than using the Koehler data over the stellar temperature range from 0.01 to 0.08 GK. The most recent evaluated stellar reactivity by Oginni et al. [12] combines both experimental results and theoretical calculations. Recommended lower and upper limits are reported from 0.01 to 10 GK, and uncertainties are a factor of 1.4 to 2.4.

We studied neutron induced reactions on ^{26}Al in campaigns at n_TOF and GELINA, using a dedicated silicon strip detection system. In both measurements, we used the same ^{26}Al sample as De Smet et al., which contains the largest concentration of ^{26}Al in the world. This sample was produced at Los Alamos National Laboratory and EC-JRC Geel [14]. It has an active area of 6×5 cm^2 and contains $2.58(12) \times 10^{17}$ atoms of ^{26}Al on a 7.5 μm thick Ni foil [11, 14]. There are small impurities of ^{10}B and ^{148}Gd, none of which cause interference with the signals expected from $^{26}\mathrm{Al}(n,\alpha)$ reactions.

n_TOF is a spallation neutron source, producing a high instantaneous neutron flux by a highly energetic (20 GeV) proton beam provided by the CERN-PS impinging on a massive Pb spallation target. The experiment was performed at the EAR-2 high flux beam line, at a flight path of about 20 m. As ^{26}Al is radioactive and only available in small quantities, this provided the ideal compromise between maximising neutron flux and maintaining good neutron energy resolution.

The detection setup at n_TOF consisted of a thin single sided silicon strip detector (SSD), 20 μm in thickness, followed by another SSD of 50 μm thickness (see Fig 1 in Ref [9]). The silicon detectors were Micron type W1 with an active area of 50×50 mm^2 and 16 strips [13]. This configuration was chosen to discriminate between α-particles and protons, and minimise background induced by prompt γ-rays and relativistic particles which are produced when the proton beam hits the spallation target (so-called γ-flash). α-particles produced by $^{26}\mathrm{Al}(n,\alpha_0)$ and $^{26}\mathrm{Al}(n,\alpha_1)$ reactions have laboratory energies of approximately 2.5 and 2.1 MeV, respectively, and are stopped in the 20 μm ΔE detectors. The $\Delta E - E$ configuration was used for the simultaneous $^{26}\mathrm{Al}(n,p)$ reaction measurement reported in a separate publication [9].

The $^{26}\mathrm{Al}(n,\alpha)$ reaction cross section was measured relative to the well known $^{10}\mathrm{B}(n,\alpha)$ reaction, by replacing the ^{26}Al sample by a ^{10}B sample, produced at STFC Daresbury Laboratory, of a well known thickness and the same active area. The areal density of this sample was determined with 5% accuracy by a proton-elastic Backscattering Spectrometry measurement at the Centro Nacional de Aceleradores (CNA, Spain). We calibrated the silicon strip detectors using a standard alpha calibration source containing ^{148}Gd, ^{237}Np, ^{241}Am and ^{244}Cm, and the αs emitted in $^{10}\mathrm{B}(n,\alpha_0+\alpha_1)$ reactions. Data were recorded using 14 bit flash-ADCs, recording the entire signal pulse shape. The development of a dedicated pulse shape algorithm allowed us to analyse signals close to the γ-flash (a signal induced by highly intense, prompt γ-radiation which is produced when the proton pulse hits the spallation target). Hence, cross sections could be determined up to neutron energies of 160 keV. A spectrum of the counts as a function of neutron energy up to 160 keV is shown in Fig. 1.

At GELINA, a pulsed neutron beam is produced by a 140 MeV electron beam impinging on a rotating U target [15, 16]. The decelerating electrons produce Bremsstrahlung which generate neutrons by photonuclear reactions on uranium. Similar to the n_TOF setup, the alpha-particles from the $^{26}\mathrm{Al}+n$ reaction were detected with two thin 20 μm SSDs placed adjacent to one another, at a flight path of about 9 m. The geometry of the GELINA setup was designed to produce a better energy resolution, e.g. using a smaller solid angle and hence producing less variation in energy loss in the target. This resulted in well separated peaks for α_0 and α_1 emission (Fig. 2 shows the deposited energy spectrum for the resonance at 41.3 keV). Data obtained during this measurement were mainly used to accurately determine the branching for alpha emission to the ground (α_0), and first excited (α_1) states in ^{23}Na, respectively (there was no measurement of the absolute cross-section with this set-up).

Figure 1 shows the count spectrum as a function of neutron energy obtained at n_TOF gated on $^{26}\mathrm{Al}(n,\alpha)$ events for (a) the resonance at 5.9 keV neutron energy, and for (b) the neutron energy range from 10 to 160 keV. Resonances identified in the $^{26}\mathrm{Al}(n,\alpha)$ reaction are underlined with solid lines. The background was estimated from the regions between resonances. The data were converted into a reaction cross section using

$$\sigma = \frac{C_{Al}}{n_{Al}\Phi\epsilon} \quad (1)$$

where C is the count rate, n is the areal density of the sample, Φ is the neutron fluence rate and ϵ is the detection efficiency. The neutron fluence spectrum at n_TOF EAR-2 has been measured in a dedicated campaign [17]. We used the $^{10}\mathrm{B}(n,\alpha)$ reference reaction to verify the energy dependence of the neutron fluence. The detection efficiency was taken into account by normalising the data to the ^{10}B sample measurement between 1 and 100 eV, where the $^{10}\mathrm{B}(n,\alpha)$ cross section is known with an uncertainty of less than 1% [18] .

Table I lists the resonance energies (E_R) and strengths ($\omega\gamma$) obtained in this work, determined as $\omega\gamma = Ak^2/(2\pi^2)$ for $^{26}\mathrm{Al}(n,\alpha_0+\alpha_1)$ reactions, where A is the area of the resonance, and k is the wavenumber. Above 100 keV, there are indications of resonances, however, the worsening neutron energy resolution precludes from providing precise resonance energies, hence only approximate values are given in the table. While there were no absolute cross-section measurements obtained at GELINA, resonance strengths (up to 50

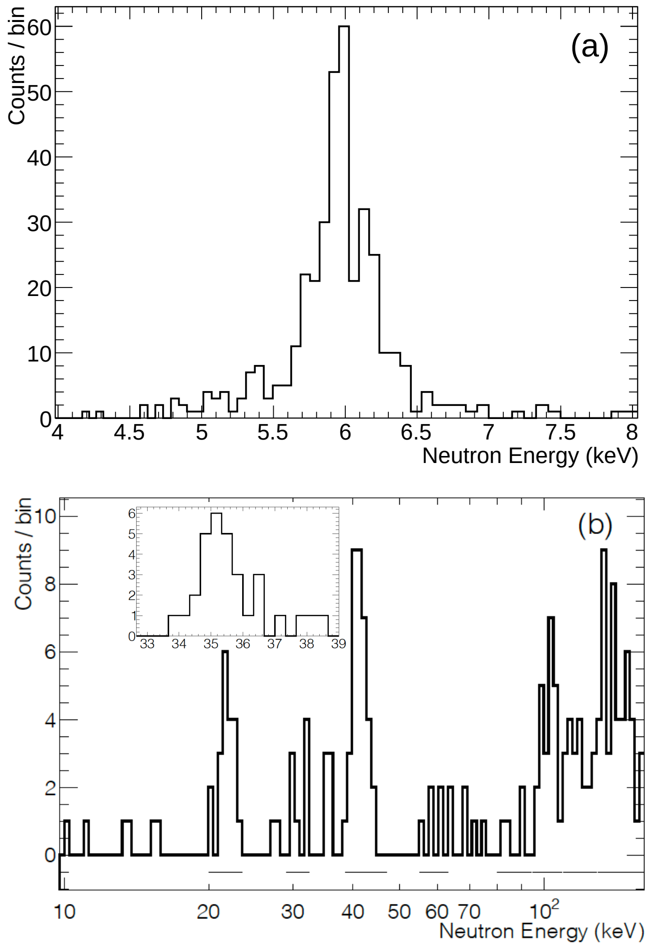

FIG. 1: (a) Count spectrum of the 5.9-keV resonance. (b) Count spectrum from 10 to 160 keV. Resonances listed in Table I are indicated by solid lines. The inset shows the count spectrum of the 35 keV-resonance obtained at GELINA used for determining the resonance strength at 35 keV, as the n_TOF neutron flux has a large absorption dip at that energy (see text for details).

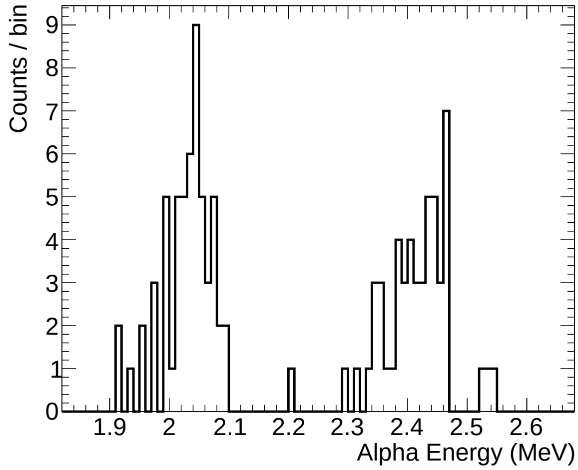

FIG. 2: α-energy spectrum measured in the 20 μm thick SSD detectors for the ^{26}Al(n,α) resonance at 41.3 keV neutron energy recorded at the GELINA time-of-flight facility. The peaks around 2.4 and 2 MeV, correspond to (n,α_0) and (n,α_1) events, respectively.

keV) measured relative to the 5.9 keV resonance were checked to confirm consistency with the n_TOF data within statistical uncertainties. For the resonance at 35 keV, the strength value in Table I was obtained by normalising the GELINA data relative to the 5.9 keV resonance, due to a strong neutron flux absorption dip around 35 keV resulting in poor statistics in the n_TOF data.

Resonance strengths are compared to results of De Smet et al. [11] and Koehler et al [10]. There is good agreement for all resonances within uncertainties with Ref. [11], while, in contrast, our strength at 5.9 keV is 1.6 times smaller than results of Ref. [10]. Uncertainties of the cross section due to systematic effects are 8%, due to uncertainties of the number of ^{26}Al nuclei in the sample (5%), the number of ^{10}B nuclei in the reference sample (5%), the energy dependence of the neutron fluence rate (2.7%) [17], and the neutron fluence normalisation between individual sample runs (3%). We have not assigned a systematic uncertainty to the background estimations, as either corrections are very small (< 2%), or the uncertainty of the correction is dominated by counting statistics.

We also determined branching ratios between α_0 and α_1 emission for four resonances (an example of a deposited energy spectrum for the resonance at 41.3 keV neutron energy is shown in Fig. 2). Results are displayed in Table I and compared to Ref. [11]. Our results agree within uncertainties at 21.9, 35.7 and 41.3 keV with [11], while there is a small difference at 5.9 keV.

We calculated stellar reactivities for a range of temperatures, using the resonance strengths $\omega\gamma$ determined up to 80 keV, and averaged cross sections from 80-160 keV neutron energy. The total stellar reactivity was calculated as

$$\begin{aligned}\langle\sigma v\rangle &= (\frac{2k_BT}{\mu})^{1/2}\sigma_{\rm th}(\frac{25.3\times10^{-6}}{k_BT[\rm keV]})^{1/2}\\ &+ (\frac{2\pi}{\mu k_BT})^{3/2}\hbar^2\Sigma_i\omega\gamma(i)\exp^{-E_R(i)/k_BT}\\ &+ (\frac{8}{\pi\mu})^{1/2}\frac{1}{(k_BT)^{3/2}}\int_{80\ \rm keV}^{160\ \rm keV}\sigma(E)E\exp^{-E/k_BT}dE\end{aligned} \tag{2}$$

where μ is the reduced mass, k_B the Boltzmann constant, T the stellar temperature, $\omega\gamma(i)$ / $E_R(i)$ are the resonance strengths /energies as determined in Table I, and $\sigma_{\rm th}$ is the cross section at thermal neutron energies (25.3 meV). The first term of the equation accounts for the contribution of the thermal cross section to the re-

TABLE I: Laboratory resonance energies E_R, resonance strengths $\omega\gamma$ and α-branching ratios $\alpha_0/(\alpha_0+\alpha_1)$ of the ^{26}Al(n,α) reaction with uncertainties due to counting statistics. Uncertainties due to systematic effects are 8%. Our data are compared to results obtained by De Smet et al. [11] and Koehler et al. [10]

This Work			De Smet et al [11]			Koehler et al. [10]	
E_R (keV)	$\omega\gamma$ (eV)	α_0/α	E_R (keV)	$\omega\gamma$ (eV)	α_0/α	E_R (keV)	$\omega\gamma(\alpha_0)$ (eV)
5.9(1)	4.25(23)	0.95(1)	5.87(2)	4.23(36)	0.87(3)	5.578	6.6(17)
21.9(2)	1.62(39)	0.96(4)	21.98(10)	1.83(27)	1.0		
31.4(4)^b	1.62(61)						
35.7(4)	3.7(10)^a	< 0.15	34.95(20)	5.98(86)	0.0		
41.3(4)	19.1(33)	0.47(5)	41.30(20)	20.2(20)	0.55(5)		
59(3)	1.8(12)						
86(4)^b	8.9(77)		85.2(8)				
≈ 105	38(11)		108.5(11)				
≈ 120	34(10)						
≈ 140	151(28)						

^{a} resonance strength determined from GELINA data normalised at 5.9 keV
^{b} resonance energy from (n,p) channel [9]

x

activity [19], assuming a $1/v$ energy dependence of the reaction cross section at low neutron energy. $\sigma_{\rm th}$ was adopted from Reference [20]. The second term refers to the contribution of resolved resonances below 80 keV to the reactivity, while the third term accounts for the unresolved contribution at high neutron energies from 80-160 keV.

Fig. 3 shows the stellar reactivities $N_A\langle\sigma v\rangle$ in units of cm^3/mol s (where N_A is the Avogadro Number) obtained in this work. The figure also shows the partial contributions of individual resonances and the unresolved region from 80-160 keV to the total reactivity. At low temperatures, the rate is determined by the first resonance at 5.9 keV, while the 41.3 keV resonance becomes more dominant between 0.2 and 0.4 GK. From 0.4 GK onwards, the unresolved cross section region from 80-160 keV makes the most important contribution. Our reactivities are reliable up to about 0.6-0.7 GK stellar temperature, while representing a lower limit for higher stellar temperatures due to the missing contribution from the cross sections for neutron energies $>$ 160 keV. Fig. 4 shows a comparison between our reactivities and previous experimental and theoretical results. Our reactivities agree well with De Smet et al. [11] up to about 0.1 GK, while being systematically higher at higher temperatures, due to the contribution of higher energy resonances to the stellar reactivity in our data (Ref [11] reports resonance strengths only below 45 keV). Compared to Koehler et al. [10], our reactivities are systematically smaller in the energy region of overlap. Theoretical and evaluated data in the Figure include reactivities from the Hauser Feshbach code NON-SMOKER [21, 22], and reactivities recommended by Oginni et al. [12], which are obtained as a combination of theoretical calculations and experimental data. From about 0.2 GK, our reactivities exceed the median values of Oginni et al., for example by about a factor 1.3 at 0.4 GK, relevant for AGB stars. The large width of the reactivity band by Oginni et al. at low stellar temperature reflects the discrepancies in the two previous experimental datasets by Koehler et al. [10] and De Smet et al. [11] .

It is evident in Fig. 4 that our new results allow to significantly reduce the uncertainty of ^{26}Al(n,α) reactivity below 0.7 GK, and are consistent with previous results obtained by De Smet et al [11]. This is also the first measurement providing cross section data above 50 keV neutron energy which allows to extend the experimental information for stellar reactivities to higher stellar temperatures. In particular at temperatures relevant to ^{26}Al synthesis in AGB stars (around 0.3-0.4 GK), our results allow to fully constrain the stellar reaction reactivity. The astrophysical reactivities obtained are higher than results by De Smet et al. and Oginni et al, which would lead to a higher destruction of ^{26}Al. While our data do not cover the full energy range relevant for ^{26}Al synthesis in massive stars (1.1-2.3 GK), we can provide a firm lower limit of the reactivity.

In summary, we measured the key destruction reaction ^{26}Al(n,α), which has a critical influence on the abundance of the cosmic γ-ray emitter ^{26}Al produced in massive and AGB stars. Our results clearly favour one of the only two existing discrepant experimental data sets. We obtain for the first time cross sections above 50 keV neutron energy, providing reliable stellar reactivities for temperatures up to about 0.7 GK. Our results suggest a higher destruction of ^{26}Al by (n,α) reactions in AGB stars, compared to using the most recently evaluated

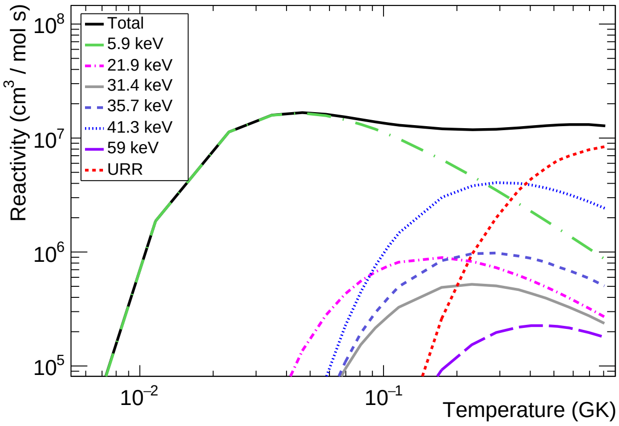

FIG. 3: Stellar reactivities obtained in this work, and the contributions of the individual resonances and the unresolved region (URR).

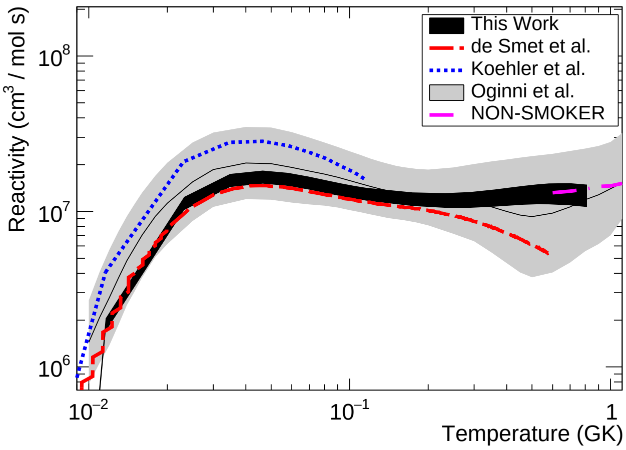

FIG. 4: Stellar reactivity compared to previous measurements and theoretical calculations. The results of this work are shown as a black band. These results are compared to experimental results by De Smet et al. [11, 23] and Koehler et al. [10], and theoretical and evaluated reactivities (NON-SMOKER [21, 22], Oginni et al. [12]). See text for details.

reactivity [12].

The authors thank P. Black (University of Edinburgh) for support in design and construction of the detection system and P. Morrall (Daresbury Laboratory) for production of the B and LiF reference samples. This work was supported by the Austrian Science Fund (FWF), project J3503, by JRC-IRMM through the EUFRAT program, by the UK Science and Technologies Facilities Council (STFC), projects ST/L005824/1 and ST/M006085/1, the European Research Council ERC-2015-STG Nr. 677497, and the Cost Action "ChETEC" (CA16117) .

[1] W. Mahoney, J.C. Ling, A.S. Jacobson, R.E. Lingenfelter, Astroph. J. **262**, 742 (1982).
[2] J. Knödlseder, Astroph. J. **510**, 915 (1999).
[3] R. Diehl, H. Halloin, K. Kretschmer, G. G. Lichti, V. Schönfelder, A. W. Strong, A. Kienlin, W. Wang, P. Jean, J. Knödlseder, J.-P. Roques, G. Weidenspointner, S. Schanne, D. H. Hartmann, C. Winkler and C. Wunderer, Nature (London) **439**, 45 (2006).
[4] M. Limongi and A. Chieffi, Astroph. J. **647**, 483 (2006).
[5] C. Iliadis, A. Champagne, A. Chieffi, M. Limongi, Astrophys. J. Suppl. S. **193**, 16 (2011).
[6] S.E. Woosley and A. Heger, Rev. Mod. Phys. 74, 1015 (2002).
[7] A. Palacios, et al., Astronomy and Astrophysics **429**, 613 (2005).
[8] D. Vescovi, et al., Astroph. J. 863, 115 (2018).
[9] C. Lederer-Woods, *et al.*, Phys. Rev. C (to be published).
[10] P. Koehler, R. Kavamagh, R. Vogelaar, Y. Gledenov, A. Popov, Phys. Rev. C **56**, 1138 (1997).
[11] L. De Smet, C. Wagemans, J. Wagemans, J. Heyse, J. Van Gils, Phys. Rev. C **76**, 045804 (2007).
[12] B.M. Oginni, C. Iliadis, A.E. Champagne, Phys. Rev. C **83**, 025802 (2011).
[13] Micron Semiconductor Ltd., http://www.micronsemiconductor.co.uk/pdf/w1.pdf.
[14] C. Ingelbrecht, A. Moens, J. Wagemans, B. Denecke, T.

Altzitzoglou, P. Johnston, Nucl. Instr. Meth. A **480**, 114 (2002).
[15] W. Mondelaers and P. Schillebeeckx, Notiziario Neutroni e Luce di Sincrotrone **11.2**, 19 (2006).
[16] A. Bensussan and J. M. Salome, Nucl. Instrum. Methods **155**, 11 1978.
[17] M. Sabate-Gilarte, *et al.* (n_TOF Collaboration), Eur. Phys. J. A **53**, 210 (2017).
[18] A.D. Carlson, et al., Nuclear Data Sheets 148 (2018) 143-188.
[19] R.L. Macklin and J.H. Gibbons, Rev. Mod. Physics **37**,166 (1965).
[20] J. Wagemans, C. Wagemans, G. Goeminne, P. Geltenbort, A. Moens, Nucl. Phys. A **696** 31 (2001).
[21] T. Rauscher and F.K. Thielemann, Atomic Data and Nuclear Data Tables, **75**, 1(2000). (online at https://nucastro.org/nonsmoker.html)
[22] T. Rauscher and F.-K. Thielemann, ADNDT 79, 47 (2001).
[23] Experimental Nuclear Reaction Data (EXFOR) Entry 22890.005, http://www-nds.iaea.org/EXFOR/22890.005.